ELSEVIER

Polymer 41 (2000) 899–906

polymer

Characterization of chemical and solid state structures of acylated chitosans

Z. Zong[a], Y. Kimura[a], M. Takahashi[a], H. Yamane[b,*]

[a]*Department of Polymer Science and Engineering, Kyoto Institute of Technology, Matsugasaki, Kyoto 606-8585, Japan*
[b]*Division of Advanced Fibro Science, Graduate School, Kyoto Institute of Technology, Matsugasaki, Kyoto 606-8585, Japan*

Received 21 December 1998; received in revised form 23 March 1999; accepted 2 April 1999

Abstract

A series of acylated chitosans were synthesized by reacting chitosan with hexanoyl, decanoyl, and lauroyl chlorides. The chemical structures of these polymers were characterized by elemental analysis, IR, ^{1}H-NMR, ^{13}C-NMR, and GPC. These results suggested that the degree of substitution was 4 per monosaccharide ring. These acylated chitosans exhibited an excellent solubility in organic solvents such as chloroform, benzene, pyridine, and THF and transparent films were obtained from these solutions. Dynamic mechanical analyses (DMA) showed that all acylated chitosans have two phase transitions in the solid state. The first transition at −10, −42, and −40°C are attributable to the glass transition (T_g) of H-, D-, and L-chitosans, respectively. The second one around 88°C may be attributed to the transition related to the structure formed by the side chains. WAXS analyses indicate that these polymers form a layered structure in solid state and the layer spacing *d* increases linearly with increasing the length of side chains.

Keywords: Acylated chitosan; Chemical structure; Solid state structure; Layered structure

1. Introduction

Chitosan is a polymer of β-1,4-linked 2-amino-2-deoxy-D-glucopyranose derived by *N*-deacetylation of chitin in aqueous alkaline medium. This polymer is known to be nontoxic, odorless, biocompatible in animal tissues, and enzymatically biodegradable. Much interest has been paid to its biomedical, ecological, and industrial applications in the past decade. However, its rigid crystalline structure, poor solubility in organic solvents and poor processability have limited it to be utilized widely. In order to resolve these problems, chemical modification of chitosan, in particular, *N*-alkylation [1,2], *N*-acylation [3,4], *O*-acylation [5], and *N*-carboxyalkylation [6], has been studied. For example, Fujii et al. [7] and Grant et al. [8] have reported on the acyl modification of chitosan reacted with long-chain acyl chloride for improving the organic solubility. Nishimura et al. [9] have also reported on phthaloylation of chitosan with phthalic anhydride. In spite of these studies, the systematic characterization of the chemical structure and properties of acylated chitosans have not been thoroughly investigated.

In this study, a series of acylated chitosans with acyl groups of different acyl lengths were prepared, and their chemical and solid state structures were characterized in detail. Particularly, the higher order structure with regard to the interplay between the flexible side chains and main chains was clarified.

2. Experimental

2.1. Materials

Chitosan from crab shell (small flake) was purchased from Nacalai Tesque, Inc., Kyoto, Japan and used without further purification. The degree of deacetylation was about 90% as determined by ^{1}H-NMR. Pyridine was dried over KOH for 48 h and then distilled. Chloroform was dried over $CaCl_2$ for 48 h and distilled. Hexanoyl, decanoyl and dodecanoyl (lauroyl) chlorides were purchased from Nacalai Tesque, Inc, Kyoto, Japan and used without purification.

2.2. Synthesis of acylated chitosans

Chitosan (3.20 g) was soaked in pyridine for one week, and the pyridine was evaporated under reduced pressure. The chitosan was then soaked again in a mixture of pyridine (90 ml) and chloroform (45 ml) for one day. The mixture was cooled to −10 ∽ −5°C in an ice–salt bath, and dodecanoyl chloride (30.6 g) dissolved in chloroform (15 ml)

* Corresponding author. +81-75-724-7824; fax: +81-75-724-7800.
E-mail address: hyamane@ipc.kit.ac.jp (H. Yamane)

0032-3861/00/$ - see front matter
PII: S0032-3861(99)00270-0

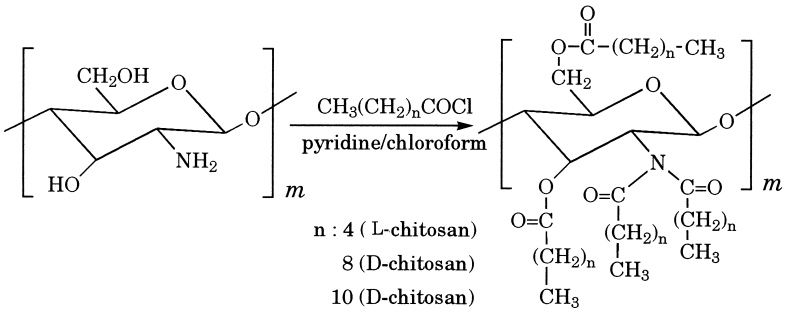

Fig. 1. Synthetic procedure of acylated chitosans.

was added dropwise in 2 h. The mixture was then stirred for 2 h at room temperature and further refluxed for 6 h. A heterogeneous aggregation of the product was observed in the mixture. The resultant mixture was poured into methanol (300 ml), and the precipitated product was filtered.The product was dissolved again in chloroform, then precipitated by pouring into methanol, filtered off, extracted in a Soxhlet extractor with methanol for 8 h, and dried in vacuum for 24 h. The drying acylated derivatives of chitosan, fresh pyridine, and chloroform were placed in a flask in the amounts described above. This procedure was repeated four times until the product was allowed to dissolve completely in chloroform. Finally, 17.32 g of light yellow product was obtained. Assuming the degree of substitution of the resultant dodecanoyl derivative to be 4, this yield corresponds to 98.0%.

Decanoyl and hexanoyl substituted chitosans were prepared in a similar manner. The hexanoyl, decanoyl and lauroyl substituted chitosans are designated as H-, D-, and L-chitosans, respectively. The synthetic procedures are represented in Fig. 1.

2.3. Measurements

Elemental analyses were done at the Elemental Analyses Center of Kyoto University.

Infrared spectra of the products were obtained with a JASCO FT/IR-5300 spectrometer. Each of the acylated chitosan was dissolved in $CHCl_3$, and the solution was cast directly on a KBr plate and solidified by slow evaporation of the solvent. Ordinary KBr pellet method was used for chitosan.

^{1}H- and ^{13}C-NMR spectra were recorded on a Bruker ARX-500 MHz spectrometer. Chitosan was dissolved in a mixed solvent of F_3CCOOD and D_2O. The acylated chitosans were dissolved in $CDCl_3$ containing 1.0% tetramethylsilane (TMS) as an internal standard.

The molecular weight and molecular weight distribution of the acylated chitosans were determined by GPC. The analyzer was composed of a Shimadzu LC-10A pump, a Shodex DEGAS KT-16 degassor, and a Sugai U-620 column oven. The eluent was $CHCl_3$ and the molecular weight was calibrated according to polystyrene standards. The concentration of solution was 0.5 mg/ml, and the injection volume was 20 μl.

Wide-angle X-ray scattering (WAXS) was recorded on a RINT 2000 diffractometer, in which the high-intensity monochromatic Ni-filtered CuKα radiation was generated at 40 kV and 30 mA.

Differential scanning calorimetry (DSC) was recorded on a DSC 3100 (MAC SCIENCE) thermal analyzer under N_2 atmosphere at a heating rate of 10°C/min and a cooling rate of 5°C/min for a sample weighing 5 mg.

Dynamic mechanical spectra were obtained on a RHEO SPECTOLER DVE-V4 with tensile mode. The heating rate

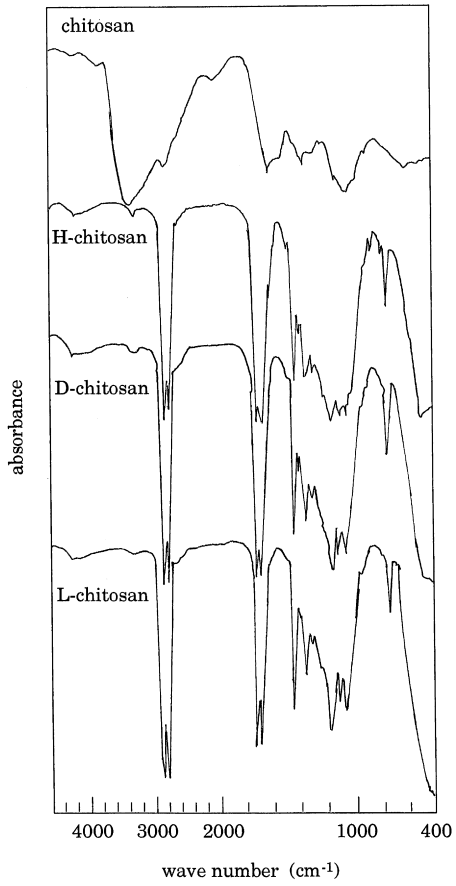

Fig. 2. Infrared spectra of chitosan and acylated chitosans.

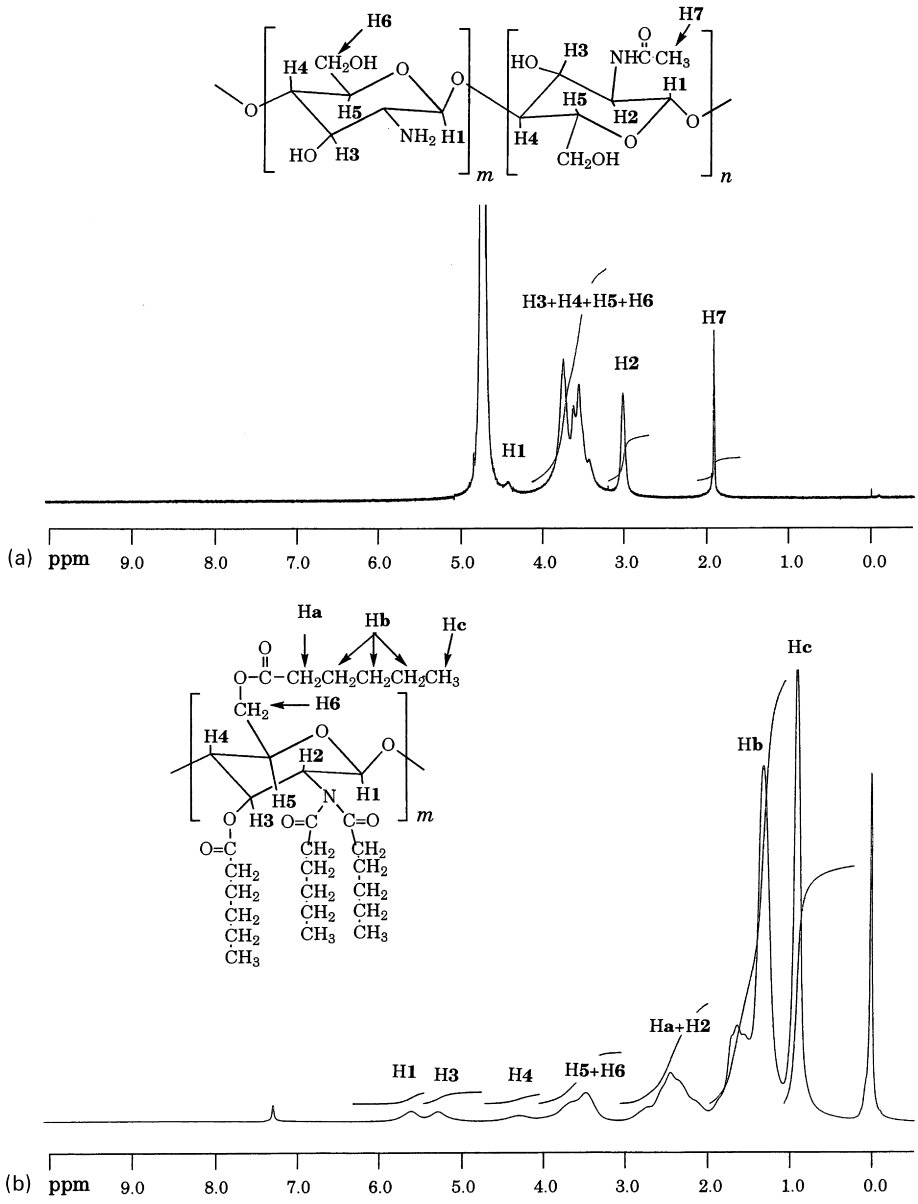

Fig. 3. ^{1}H-NMR spectra of: (a) chitosan in F_3CCOOD/D_2O; and (b) H-chitosan in $CDCl_3$.

was 2°C/min, and the sample size was 20×5 mm with a thickness of $0.4 \sim 0.7$ mm.

3. Results and discussion

3.1. Characterization of acylated chitosans

The infrared spectra of chitosan and its acylated derivatives are shown in Fig. 2. The characteristic absorption at $3000 \sim 4000\ cm^{-1}$ (OH, NH_2) is shown in chitosan while absent in the acylated chitosans which show new peaks at $1716\ cm^{-1}$ (C=O of $N(COR)_2$) and $1747\ cm^{-1}$ (C=O of OCOR). The peaks at $2924\ cm^{-1}$ (ν_{as} CH_2), $2854\ cm^{-1}$ (ν_s CH_2), $1464\ cm^{-1}$ (δ CH_2), $1182\ cm^{-1}$ (twisting vibration of CH_2) are stronger and sharper in the latter. These results suggest that all four hydroxy and amino groups on the monosaccharide structure of the chitosan were fully acylated and the amino group was converted to imide group.

The ^{1}H-NMR spectra of the original chitosan in F_3CCOOD/D_2O and the H-chitosan in $CDCl_3$ are compared in Fig. 3. While chitosan shows a singlet at 3.0 ppm (H2) and multiplets at $3.5 \sim 3.8$ ppm (H3, H4, H5, 2 H6) corresponding to the ring methine protons together with a singlet at 1.95 ppm (H7) and a small signal at 4.4 ppm (H1). The latter signals are due to the *N*-acetyl glucosamine units having survived the saponification of chitin. From the integration the acetyl content was calculated to be 10%. H-chitosan shows signals at 5.6 (H1), 5.3 (H3), 4.25 (H4),

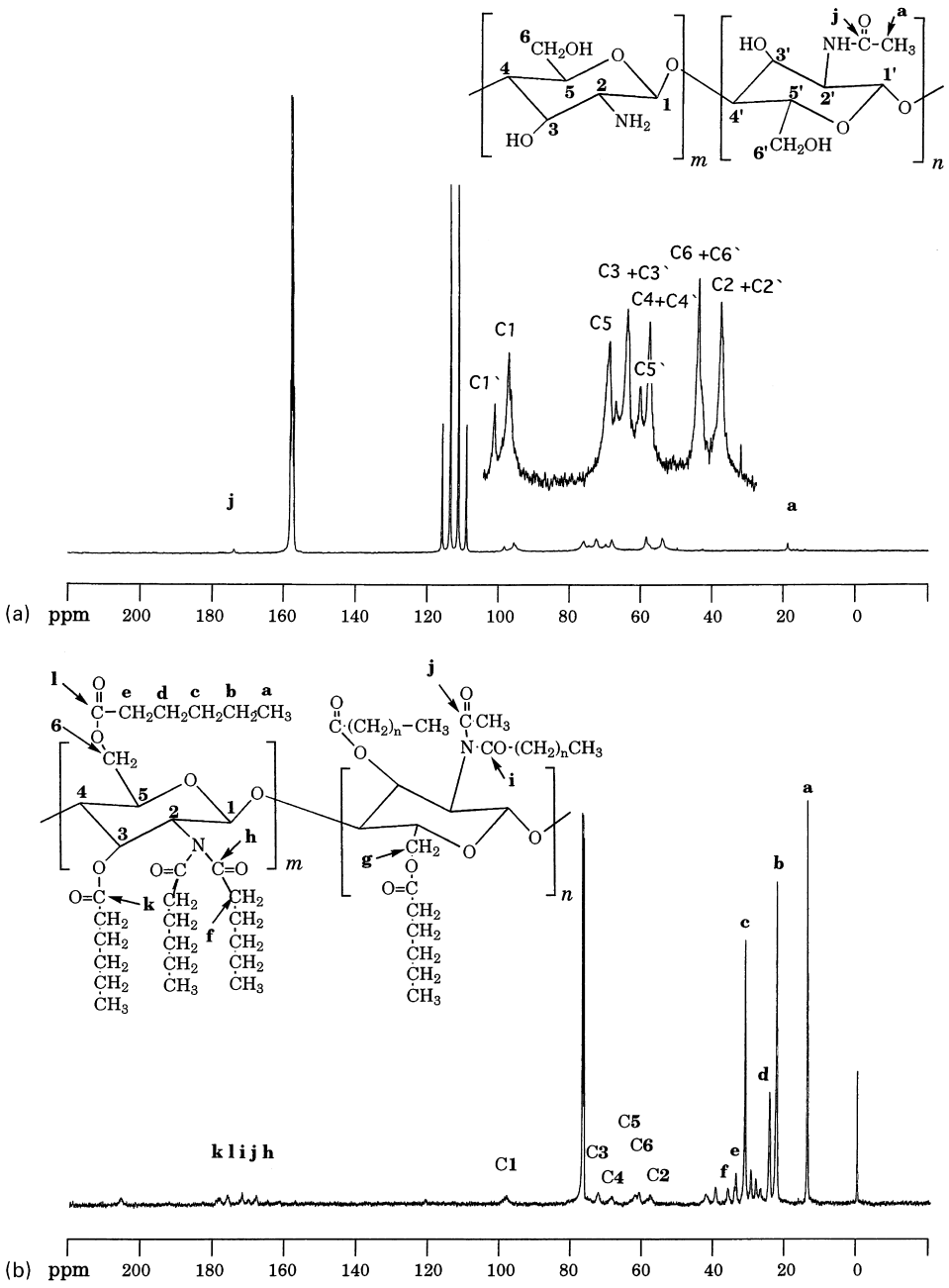

Fig. 4. ^{13}C-NMR spectra of: (a) chitosan in F_3CCOOD/D_2O and (b) H-chitosan in $CDCl_3$.

3.3 ~ 3.8 (H6, H5), 2.75 (H2) (ppm) due to the protons of the polysaccharide ring together with the signals at 2.45 ($-CO-CH_2-$), 1.35 ~ 1.65($-CH_2-$) and 0.9 ($-CH_3$) (ppm) which are assigned to the hexanoyl chains. The chemical shifts of the ring protons of the H-chitosan shifted to downfield because of the electron-withdrawing effect of the acyl substituents. Furthermore, the integral ratio of the signals of hexanoyl groups to those of the chitosan structure suggested that the degree of substitution with acyl groups is 4 per monosaccharide ring, i.e. both amino and amide groups of the original chitosan are imided.

Fig. 4 shows the ^{13}C-NMR spectra of H-chitosan in $CDCl_3$ as compared with the original chitosan in F_3CCOOD/D_2O. In the latter, the signals due to C1 and C1′ carbons, directly attaching to two oxygen atoms, are found at 95.2 and 98.2 ppm which are significantly lower magnetic field compared with the signals of the remaining five carbons. As there are two different units in the structure of chitosan, the signals at 54 (C2 + C2′), 73 (C3 + C3′), 67.6 (C4 + C4′), 70.5 (C5′), 75.8 (C5) and 58 (C6 + C6′) (ppm) are detected, although the signals in the lower fields are split into two due to the different saccharide structures. The peaks at 19 and 174 ppm are assigned to the methyl and carbonyl carbons of the acetyl groups of the

Table 1
Elemental analyses, molecular weights and distributions of chitosan and acylated chitosans

	Calcd.			Found			$M_n(\times 10^5)$	M_w/M_n	P_n
	C%	H%	N%	C%	H%	N%			
Chitosan	44.7	6.8	8.7	43.2	7.0	7.6	–	–	–
H-chitosan	65.1	9.2	2.5	65.9	9.3	2.0	2.77	1.7	500
D-chitosan	71.0	10.7	1.8	71.3	10.9	1.6	3.11	2.6	400
L-chitosan	72.9	11.1	1.6	73.1	11.1	1.4	4.03	2.4	453

N-acetylglucosamine units, respectively. For the H-chitosan, the signals shown at 58 (C2), 62 (C6), 69 (C4), 73 (C3), and 99 (C1) (ppm) are attributed to the carbons in the polysaccharide structures. Note that a single signal is shown for the glycoside carbon (C1) because both the amino and amide units of the original chitosan are fully imided. The signals of the β-ϵ carbons of the hexanoyl groups are shown at 14.2 (a), 23.2 (b), 32.0 (c), 25.0 (d) as single signals while the signals of α-CH_2 are split into 7 peaks, at 30.0, 27.0, 28.5, 34.2, 36.0, 40.0, and 43 ppm corresponding to the hexanoyl groups in different environments. The methyl carbon signal of the acetyl groups may superimpose with one of the above signals. The signals shown at 179, 177, 173, 171 and 169 ppm are assigned to the carbonyl carbons, although the assignment of each signal was not possible to elucidate completely. These evidences obviously support the fully acylated chitosans in which the amino and amide groups of the original chitosan were converted to imides.

The results of elemental analysis of the chitosan and its acylated products are listed in Table 1. The experimental results are compared with the values calculated, assuming that the degree of substitution (DS) is 4. The nitrogen percentages of the D- and L-chitosans are in reasonable agreement with the calculated values, while the nitrogen value of H-chitosan is a little lower than the calculated value. The nitrogen percentage of chitosan is lower by about 1.0% and the hydrogen percentage is higher than the calculated value probably due to the absorption of water.

The molecular weights, molecular weight distribution, and the degree of polymerization of the acylated chitosans are also listed in Table 1. The chitosans acylated with longer acyl chlorides have higher molecular weights. Assuming the degree of substitution is 4 for all of the derivatives, the degrees of polymerization of the acylated chitosans are in the range of 400 ~ 500. Since the acylated chitosans showed a single symmetrical curve without tailing in their GPC chromatogram, they involved no small molecule. These results indicate that the acylation did not alter the chain length of the original chitosan.

3.2. Properties of the acylated chitosans

In contrast to the chitosan, all of the acylated chitosans showed an excellent solubility in common organic solvents (Table 2) such as halogenated hydrocarbons and aromatic solvents, but poor solubility in polar solvents. Thin transparent films could be obtained by casting their solutions in $CHCl_3$. While the chitosan film is rigid and tough, the films of the acylated chitosans are softer and become even more sticky and elastic at room temperature with increasing chain length of the acyl substituents.

DSC thermograms of the chitosan and acylated chitosans are shown in Fig. 5. The chitosan shows a broad endothermic peak around 84°C and a decomposition peak at 298°C. The former endothermic peak may be due to the vaporization of the water contaminant which can not be removed even after the chitosan sample was dried at 90°C for 48 h in vacuum, as supported by its elemental analysis data. The T_g of D- and L-chitosans are detected at −43 and −37°C, respectively, but no obvious glass transition was observed for H-chitosan. The exothermic peaks of H-, D-, and L-chitosans at 225, 246 and 255°C, respectively, correspond to their thermal decomposition. The accumulated small

Table 2
Solubility and processability of chitosan and acylated chitosans (◎: dissolved easily, ○: dissolved, Δ: swelling, ×: not dissolve)

	Solubility										Cast film	
	$CHCl_3$	CH_2Cl_2	C_6H_6	$C_6H_5CH_3$	Pyridine	THF	Dioxane	DMF	DMAc	DMSO	Appearance	
Chitosan	×	×	×	×	×	×	×	×	×	×	Transparent[a]	Brittle
H-chitosan	◎	◎	◎	○	○	○	Δ	Δ	Δ	Δ	Transparent[b]	Soft
D-chitosan	◎	◎	○	○	○	○	Δ	Δ	Δ	×	Transparent[b]	Tacky elastic
L-chitosan	◎	◎	○	○	○	○	Δ	Δ	Δ	×	Transparent[b]	Sticky elastic

[a] Solvent: water/acetic acid.
[b] Solvent: chloroform.

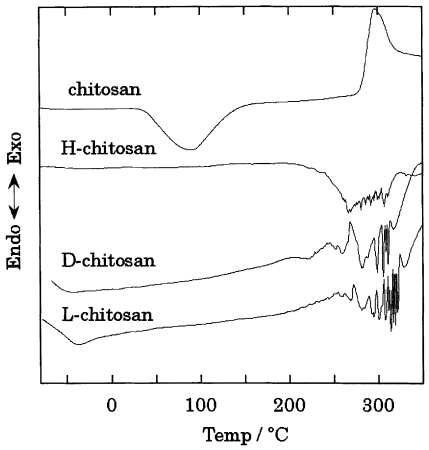

Fig. 5. DSC thermograms of chitosan and acylated chitosans.

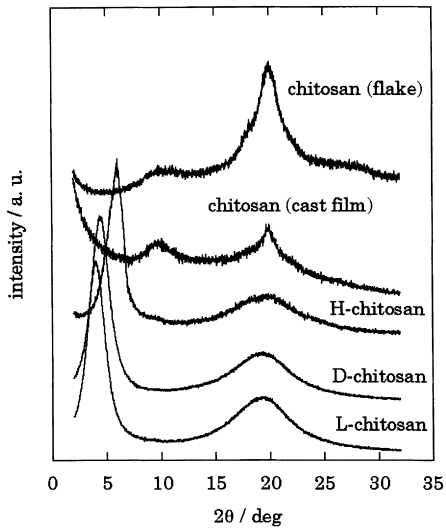

Fig. 7. WAXD patterns of chitosan and acylated chitosans.

peaks suggest that the decomposition caused disintegration into tiny fragments. Grant et al. [8] also reported that chitosan with a degree of deacetylation of 86.4% and its lauroyl derivative show the exothermic decomposition peaks at 322 and 217°C, respectively. From these evidences we conclude that the thermal stability should decrease by introduction of the acyl groups. The acylated chitosans are stable below 225°C. Introduction of lateral substituents or flexible units into polysaccharide structures should disrupt the crystalline structure of chitosan, especially through the loss of the hydrogen bonding.

Krigbaum et al. [10] incorporated the flexible segments in a rigid polyester to reduce its crystal–nematic transition temperature. Ballauff et al. [11,12] attached flexible side chains to the stiff backbone of aromatic polyesters and polyimides to lower the melting point of such polymers. Ballauff [13] also theoretically derived the conclusion that the presence of flexible side chains in these polymers profoundly altered the phase diagrams as compared to the rigid rod model. This alteration caused thermal instability of the derivatives because of the increased chain mobility. The acylated chitosans also attained solubility in charge of losing thermal stability.

Dynamic mechanical spectra of the chitosan and acylated chitosans are shown in Fig. 6. The storage modulus of the acylated chitosans is much lower than that of the chitosan over the whole temperature range of measurement and is affected greatly by the change of temperature. The storage modulus of the acylated chitosans decreases with increasing number of carbon atoms of the acyl substituents. The tan δ spectra show two phase changes for the acylated chitosans. The lower tan δ peaks at −10, −42, and −40°C correspond to the T_g of H-, D- and L-chitosans, respectively. This result is almost correspondent with the DSC results of D- and L-chitosans. The second transition temperature around 88°C is independent of the length of side chains, while the tan δ value corresponding to it increases with increasing number of carbon atoms of side chains. The similarity of dynamic mechanical spectra suggests that there are similar phase transitions in the solid state of the acylated chitosans.

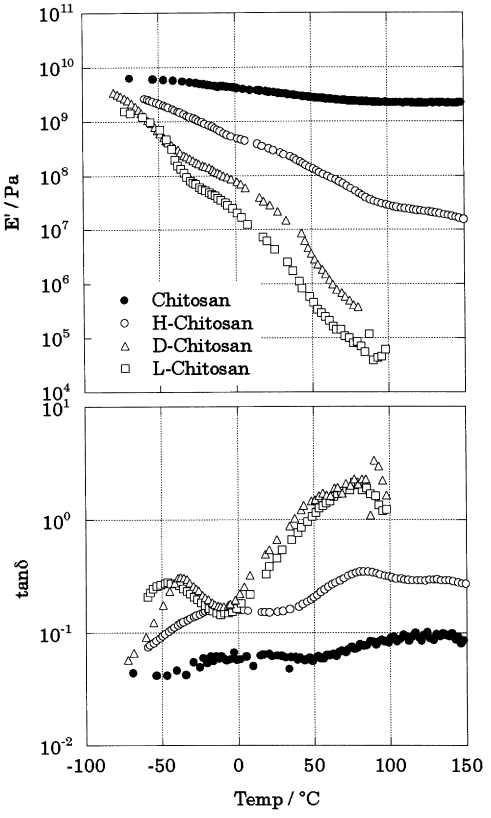

Fig. 6. Dynamic mechanical spectra of chitosan and acylated chitosans.

3.3. Solid state structures of the acylated chitosans

Fig. 7 shows the WAXS profiles of the acylated chitosans as compared with that of chitosan. Samuels [14] reported

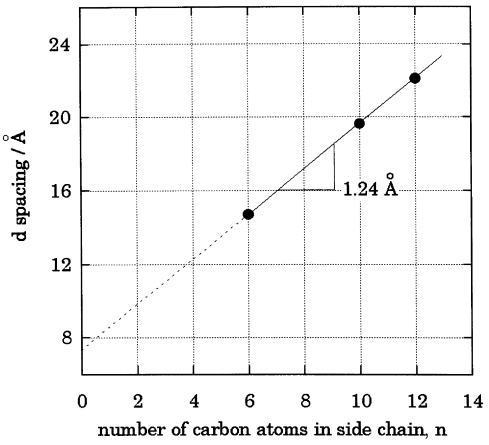

Fig. 8. *d*-spacing of acylated chitosans calculated from the peaks at low Bragg angles as a function of the number of carbon atoms of the side chain.

that chitosan has two distinct crystal forms I and II. The form I crystal is orthorhombic having an unit cell of $a = 7.76$ Å, $b = 10.91$ Å, and $c = 10.30$ Å. The strongest reflection falls at $2\theta = 11.4°$, which is assigned to (100) reflection. The form II crystal is also orthorhombic having an unit cell of $a = 4.4$ Å, $b = 10.0$ Å, and $c = 10.3$ Å (fiber axis). The strongest reflection appears at $2\theta = 20.1°$, which also corresponds to the (100) reflection. As shown in Fig. 7, the original chitosan in flake state shows the strongest reflection at $2\theta = 20°$ while the cast film prepared from its solution in water/acetic acid shows a weak reflection at $2\theta = 20°$ and a strong reflection at $2\theta = 10°$. These observations should be explained by the partial change from crystal form II with constrained chain conformation to form I having a more extended chain structure when chitosan is once dissolved in dilute aqueous acetic acid and cast into film. The acyl substituted chitosans show a broad reflection at around $2\theta = 20°$ together with a strong reflection at $2\theta = 2 \sim 6°$. The former reflection indicates that the main

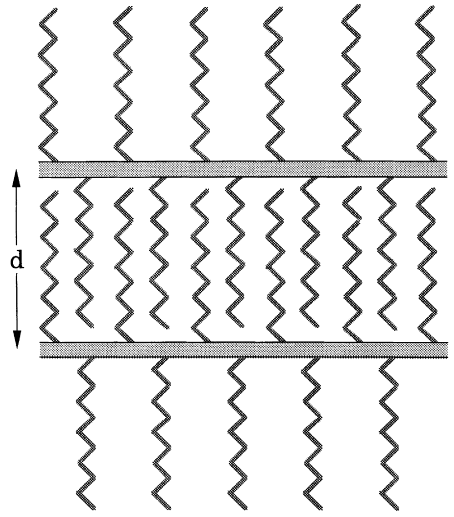

Fig. 9. Speculated layered structure of acylated chitosans.

polysaccharide chains cannot keep *a*-axis (100) reflection after losing hydrogen bonding which prevailed in original chitosan structures. The latter suggests a new type of ordering structure. The *d*-spacing of this reflection of each derivative is plotted in Fig. 8 as a function of the number of the carbon atoms of the acyl substituents (*n*). A linear relationship is obtained between the *d*-spacing and *n* from which the increment in the *d*-spacing for each CH_2 unit is found to be 1.24 Å. This value is in reasonable agreement with the theoretical bond length of CH_2 unit (1.27 Å). Therefore, the side chains are interdegitated with each other forming a layered structure with the main chains extended (Fig. 9). Similar results have been reported by Lee et al. [15], who studied the higher order structures of a series of comblike semiflexible polymers, in which the alkyl side chains were located on the ring of hydroxypropylcellulose (HPC). They found that the *d*-spacing increment per each CH_2 was 1.66 Å, much greater than the theoretical value of 1.27 Å and proposed the higher order structure in which the side chains were not completely interdegitated and tilted at some angle to the main chains. Ballauff et al. [11,16] and Rodriguez-Parada [17] also found a similar linear relationships between the layer spacing *d* and the length of the hydrocarbon chains in their studies on the aromatic polyesters and polyamides having long alkoxy side chains and observed that these kinds of polyesters have layered mesophase and layered crystalline structures at room temperature. Our results indicate that the present acylated chitosans have only one layered structure at room temperature.

Even though the main chains are extended and form layered stacks, they may be disordered tridimensionally and give rise to a broad reflection at $2\theta = 20°$. This may be (1) the main chains of the polysaccharide will not be all coplanar and have different angles of rotation relative to each other due to the ether linkage, while the main chains are constrained under hydrogen bonds in chitosan structures, (2) both *N*-acetylglucosamine units are involved in the polysaccharide sequence to retard crystallization, and (3) the disordered packing of the side chains having rotational freedom will prevent the occurrence of well-defined reflections for main chains. These effects can explain a low degree of ordered packing of main chains.

4. Conclusions

Three kinds of acylated chitosans were synthesized by reacting chitosan with hexanoyl, decanoyl, and lauroyl chlorides. The degree of substitution was 4 per monosaccharide ring. The acylated chitosans exhibited excellent solubility in common organic solvents and good film formability. The thermal stability of these polymers was lower than that of chitosan with losing hydrogen bonding. The storage modulus of the acylated chitosans was much lower than that of chitosan and was affected greatly by the temperature change. The similar dynamic mechanical

behavior among the three derivatives suggested a common phase transition in solid state. The acyl side chains in H-, D-, and L-chitosans should assemble into a similar layered structure. The layer spacing d increased linearly with increasing length of the acyl substituents.

References

[1] Hall LD, Yalpani M. J Chem Soc, Chem Commun 1980;:1153.
[2] Yalpani M, Hall LD. Macromolecules 1984;17:272.
[3] Hirano S, Ohe Y, Ono H. Carbohydr Res 1976;47:315.
[4] Moore GK, Goerge AF, Int. J Biol Macromol 1981;3:292.
[5] Grant S, Blair HS, Mckay G. Makromol Chem 1989;190:2279.
[6] Muzzarelli RAA, Tanfani F. Pure Appl Chem 1982;54:2141.
[7] Fujii S, Kumagai H, Noda M. Carbohydr Res 1980;83:389.
[8] Grant S, Blair HS, McKay G. Polym Commun 1990;31:267.
[9] Nishimura SI, Kohgo O, Kurita K, Kuzuhara H. Macromolecules 1991;24:4745.
[10] Krigbaum WR, Hakemi H, Kotek R. Macromolecules 1985;18:965.
[11] Ballauff M, Schmidt GF. Makromol Chem, Rapid Commun 1987;17:973.
[12] Wenzel M, Ballauff M, Wegner G. Makromol Chem 1987;188:2865.
[13] Ballauff M. Macromolecules 1986;19:1366.
[14] Samuels RJ. J Polym Sci, Polym Phys Ed 1981;19:1081.
[15] Lee TL, Pearce EM, Kwei TK. Macromolecules 1997;30:8233.
[16] Ballauff M, Schmidt GF. Mol Cryst Liq Cryst 1987;147:163.
[17] Rodriguez-Parada JM, Duran R, Wegner G. Macromolecules 1989;22:2507.